

# A Novel Split-Ring Resonator and Voltage Multiplier Based Rectenna Design for 900 MHz Energy Harvesting Applications

Merih PALANDOKEN, Cem GOCEN, Adnan KAYA,  
Fethullah GUNES, Cem BAYTORE, Fatih Cemal CAN

Electrical and Electronic Engineering Dept., Izmir Katip Celebi University, Izmir, Turkey

merih.palandoken@ikc.edu.tr, gocencem@gmail.com,  
{adnan.kaya, fethullah.gunes, cem.baytore, fatihcemal.can}@ikc.edu.tr

Submitted March 26, 2018 / Accepted June 14, 2018

**Abstract.** This paper proposes a novel rectenna design for the compact RF energy harvesting system operating at 900 MHz. The rectenna design is based on a probe fed split-ring resonator on an elliptical slotted ground plane and an RF-DC rectifying circuit in the form of Villard voltage doubler circuit. The energy harvesting antenna is numerically modeled and fabricated on a 1.524 mm thick Rogers RO4003C substrate with a compact overall size of 81.25 mm × 87.5 mm ( $\lambda_0/4.1 \times \lambda_0/3.8$ ). The measured reflection coefficient indicates the proposed energy harvesting antenna to operate at 890 MHz with 51.3 MHz bandwidth covering GSM 900 band. As an RF-DC rectifying electronic circuit, a one stage voltage doubler circuit based on zero bias Schottky barrier diode in conjunction with the inductive impedance matching and  $\lambda/4$  impedance transformer circuits has been designed. The DC voltage of nonlinear RF rectifier circuit is obtained as 1.7 V at the output load for  $-11$  dBm input power level. The measured and simulated results confirm the proposed rectenna system to have a technical potential for the operation of low power and low voltage electronic devices.

## Keywords

RF energy harvesting, rectenna, microstrip antenna, RF-DC conversion, voltage multiplier

## 1. Introduction

In recent years, there has been a rapid growth in many wireless communication applications such as wireless sensor networks and IoT [1]. Since these wireless applications consist of a large number of low power, low voltage operating sensors, ubiquitous and continuous supply of energy is essential for their reliable operation [2]. As the power demand increases, the need for the alternative energy sources has become important. In this regard, energy harvesting from the ambient environmental energy sources

and corresponding power conversion to the usable DC voltage levels is the key solution [3]. With the technological and scientific improvements, RF energy harvesting technique becomes more efficient. In the modern environment, there are multiple external ambient RF energy sources at different operating frequencies radiating RF power in all directions. These sources are TV and radio broadcast stations, mobile phone base stations, cellular phones, and wireless Local Area Network (LAN) transceivers. RF energy harvesting system targets the continuous gathering of RF energy from the external ambient sources for the purpose of providing sufficient DC power to the low power electronic equipment.

In RF energy harvesting technique, the radio signals with the frequency range from 300 GHz to as low as 3 kHz are used as the RF input source to be rectified into the permissible DC voltage level [2]. Therefore, the diverse frequency spectrum opportunity for the RF energy harvesting is existing to energize the low power devices without the regular need of replacing batteries [4]. In addition, there is an active research potential in the investigation of the multiple alternative ways to scavenge energy from the environment and convert into the DC electrical energy to energize the low power devices [5].

The basic RF energy harvesting system block diagram is shown in Fig. 1. RF energy harvesting system includes the receiving antenna, matching network and rectifying circuit. The environmentally freely available RF energy is conveniently captured by the receiving antenna and converted into the permissible DC power level by the voltage rectifier circuitry. In this system, the receiving antenna is utilized for gathering RF signals from the environment in every location in space. Antenna physical dimensions, high directive gain, and good radiation pattern are the main aims of the antenna design. Another important part of the system is the matching network. The crucial task of matching network is to reduce the reflection and transmission losses from the receiving antenna to the RF rectifier electronic circuit and increase the output voltage of the rectifier circuit

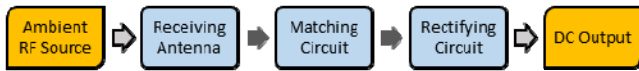


Fig. 1. RF energy harvesting system block diagram.

[6]. The input impedance of the RF rectifier electronic circuit is different from the antenna input impedance ( $50 \Omega$ ), thus the impedance matching is therefore required to transfer the maximum available power to the load. The last important part of the system is the RF rectifier electronic circuit. Rectifier circuit has to be capable of converting an input RF signal into a considerable DC voltage level. The different topologies of the rectifier circuits have been discussed in the literature for RF energy harvesting systems such as Greinacher rectifier, Villard voltage rectifier and Dickson rectifier [7–9].

In 2014, the study presented by Lu et al. has provided an overview of RF energy harvesting networks including system architecture, RF energy harvesting techniques, and existing applications [2]. A high gain printed dual-band meandered dipole antenna has been proposed for RF energy harvesting applications in the GSM-1800 and WiFi bands by Sarma et al., in 2016 [10]. The antenna has been designed to achieve maximum gain in dual band. In 2016, the research work on design, analysis, and optimization of RF energy harvesting system for WLAN source operating at 2.4 GHz and 5.8 GHz has been presented by Munir et al. [7]. The researchers have achieved to provide 1.3 mW power across  $10 \text{ k}\Omega$  load, which could be enough to energize the low power devices for the received RF power of 5 dBm. In 2017, a wideband slot rectenna has been designed for the wireless power transmission operating at the WLAN 2.45 GHz band, by Chang et al. [11]. The simulated maximum system efficiency of 73.7% has been achieved. In [12], Zakaria et al. presented energy harvesting system based on 3dBi helical monopole antenna operating at 902 MHz in ISM band with output DC voltage of 200 mV and 1.08 V for the RF input power level of  $-22.5$  and  $-11$  dBm, respectively. Different energy harvesting antenna designs operating at higher frequencies [13–17] and alternative compact antenna design techniques, which can be utilized in the energy harvesting system are investigated in [18] in addition to the electrically small antennas based on split-ring resonators formed artificial magnetic material unit cells in [19–21].

In this paper, a compact rectenna design is proposed for the energy harvesting applications in 900 MHz band. The receiving antenna section of the proposed rectenna is modeled on 1.524 mm thick Rogers RO4003C substrate for the numerical computations and verified by the experimental results. The input impedances of the proposed antenna and rectifying circuit are matched using the series inductor and quarter wavelength matching networks. Villard voltage doubler rectifier circuit has been used for RF to DC conversion. The proposed antenna geometry and rectifying circuit design principle are explained in Sec. 2. The numerical computation and experimental results are presented in Sec. 3. The concluding remarks are conducted in Sec. 4.

## 2. Rectenna Configuration

The design and analysis of RF energy harvesting system for GSM-900 frequency band as a whole complete model are explained in this section with the design details of energy harvesting antenna, AC-DC rectifier RF electronic circuit, and impedance matching network.

### 2.1 Energy Harvesting Antenna

The top and bottom layers of the energy harvesting antenna model are shown in Fig. 2 along with the fabricated antenna prototype using Rogers RO4003C substrate. The proposed antenna is modeled and RF performance parameters are numerically calculated in FIT based commercial 3D numerical computation program CST Studio Suite [22]. The substrate material is selected to be 1.524 mm thick Rogers RO4003C substrate with the dielectric constant of 3.38 and loss tangent of 0.0027. The physical size of the energy harvesting antenna is  $L1 \times L2$  ( $81.25 \times 87.5$  mm). The top side of the proposed antenna geometry is structured in the form of split ring resonator (SRR) which is directly fed through the probe feeding technique from the bottom side of the substrate. The bottom side of the proposed antenna geometry is however in the form of a slotted ring with the elliptical metallic section in the inner and outer sides. In the antenna design principle,

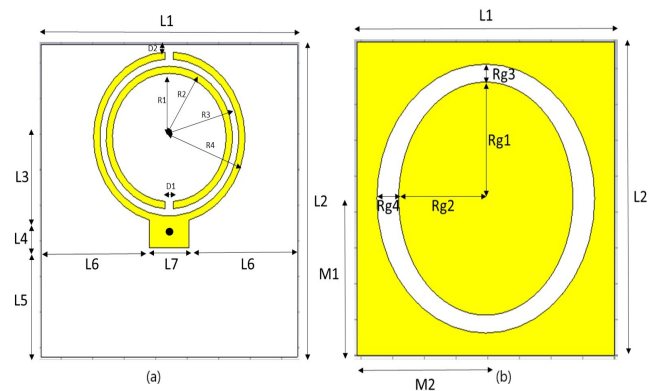


Fig. 2.a. Proposed energy harvesting antenna model with design parameters: (a) top and (b) bottom views. (The relevant dimensions are (in mm);  $R1=18$ ,  $R2=20$ ,  $R3=22$ ,  $R4=24$ ,  $D1=2.5$ ,  $D2=2$ ,  $L1=81.25$ ,  $L2=87.5$ ,  $L3=23$ ,  $L4=8.2$ ,  $L5=30.1$ ,  $L6=34.375$ ,  $L7=12.5$ ,  $M1=43.75$ ,  $M2=40.625$ ,  $Rg1=32.5$ ,  $Rg2=27.5$ ,  $Rg3=5$ ,  $Rg4=6.5$ ,  $\bullet$  is feeding point)

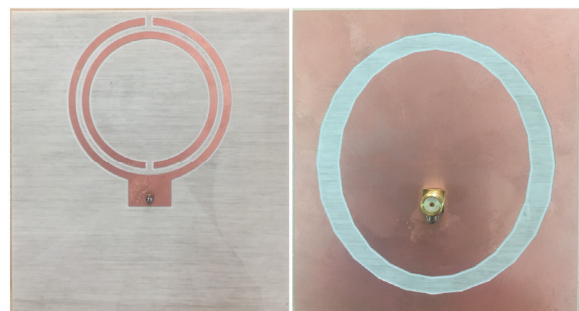


Fig. 2.b. The fabricated prototype of the proposed energy harvesting antenna.

the geometric parameters of directly fed SRR are optimized for the SRR formed radiator to be excited in the second higher order mode with the electrical near field coupling to the resonant elliptical slot in the ground plane. The geometric parameters of inner and outer rings of the top side of the proposed antenna in addition to those of the elliptically slotted ground plane are parametrically studied and optimized in order to have the resonance frequency at 900 MHz.

### 2.2 Rectifying Circuit

The rectifying circuit has an important systematic effect on the energy harvesting system’s performance due to the primary objective of highly efficient conversion of RF power into DC power. The targeted rectifying circuit has to be designed with the operational capability of possibly high conversion efficiency in addition to the unidirectional current flow and low RF transmission loss. A one stage voltage doubler circuit based on zero bias Schottky detector diode, SMS 7630 Skyworks, in conjunction with inductive impedance matching and  $\lambda/4$  impedance transformer circuits has been designed with the numerical model in Ansoft Designer [23]. The numerical model is shown in Fig. 3.

The lumped circuit element values are listed in Tab. 1. In Fig. 3, the RF terminal voltage at the energy harvesting antenna input is designated as  $V_{sig}$ . Because of the nonlinear RF analog circuit feature of the RF-DC rectifier circuit, the DC output voltage is highly dependent on the input RF power level, operating frequency, and DC load. The RF-DC voltage doubler circuit is designed to be matched to the antenna input impedance of  $50 \Omega$  for  $1 \mu W$  ( $-30$  dBm) input power level for  $50 \text{ k}\Omega$  DC load with the reflection coefficient of  $-30$  dB. However, the maximum RF-DC conversion efficiency of 75% has been obtained at  $-11$  dBm input power level for the RF-DC rectifier circuit. The Spice component design parameters of zero bias Schottky detector diode, SMS 7630 [24] are used in the nonlinear circuit simulation and listed in Tab. 2. The DC load resistance is quite similar to the input resistance of the commercial temperature sensor, KY-028 Digital Temperature Sensor [25].

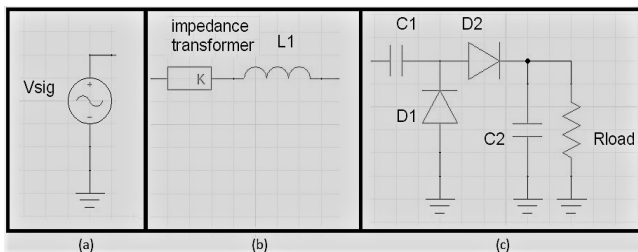


Fig. 3. Configuration of the proposed rectifying circuit: (a) Input RF power, (b) matching circuit, (c) Villard doubler circuit with DC load (temperature sensor).

Z line	L line	L1	C1	C2	R load
77.45 $\Omega$	44.5 mm	150 nH	1.5 nF	5.6 nF	50 $\text{k}\Omega$

Tab. 1. Design parameters of proposed rectifying circuit with DC load.

Is (A)	$5 \times 10^{-6}$	XTI	2
Rs ( $\Omega$ )	20	Fc	0.5
N	1.05	Bv (V)	2
TT (sec)	$10^{-11}$	IBV (A)	$10^{-4}$
Cj0 (pF)	0.14	Vj (V)	0.34
M	0.4	EG (eV)	0.69

Tab. 2. SMS 7630 spice component parameters [21].

### 3. Numerical and Experimental Results

The proposed antenna design has been modeled in 3D commercial high frequency simulator CST Studio Suite and fabricated using Rogers RO4003C substrate for the performance measurement. The fabricated prototype of the optimized numerical model is measured with (Signal Hound USB-SA124B Spectrum Analyzer and USB-TG124A Tracking Generator). The numerical and experimental results of reflection coefficient (S11) are shown in Fig. 4. The numerically computed resonance frequency is 900 MHz with the return loss of 21 dB and 10-dB bandwidth of 34.6 MHz. The resonance frequency of the fabricated prototype is 890 MHz with the return loss of 21 dB and 10-dB bandwidth of 51.3 MHz.

Numerical computations are done for the optimization of the proposed energy harvesting antenna to have the resonance frequency at 900 MHz. As deduced from the parametric studies, two of the most significant parameters affecting the resonance frequency and operation bandwidth are  $R_{g1}$  and  $R_{g2}$  of the slotted elliptical ring in the ground plane. The input reflection coefficient results indicating the effect of  $R_{g1}$  and  $R_{g2}$  parameter changes on the resonance frequency and the operation bandwidths of the proposed antenna design are presented in Fig. 5.

As deduced from Fig. 5, the increasing perimeter of the slotted elliptical ring in the ground plane results not only the resonance frequency to be lower but also to prevent the second resonance frequency to emerge in the operation band due to the near field coupling to the radiating SRR. Therefore, both radiating elements have to be parametrically studied to set the antenna resonance frequency to 900 MHz.

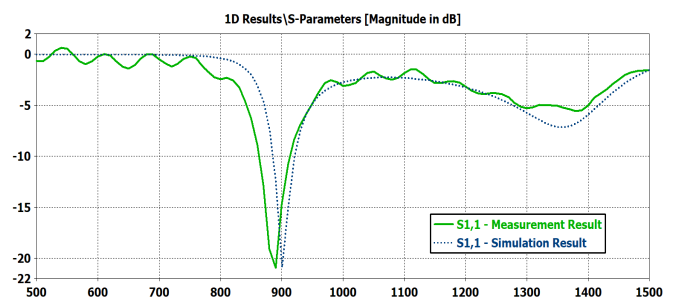


Fig. 4. The input reflection coefficient (S11) of the proposed energy harvesting antenna (simulation and measurement results).

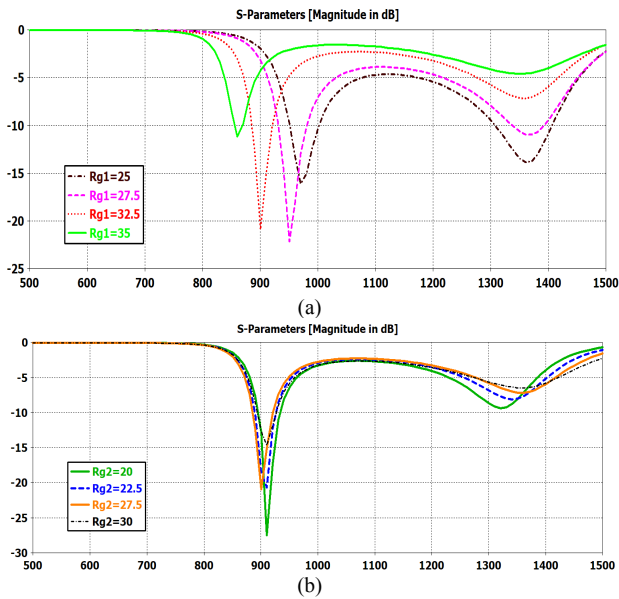


Fig. 5. The input reflection coefficient (S11) of the proposed energy harvesting antenna with the different variables; (a) Effect of Rg1 (Rg2 = 27.5 mm), and (b) effect of Rg2 (Rg1 = 32.5 mm).

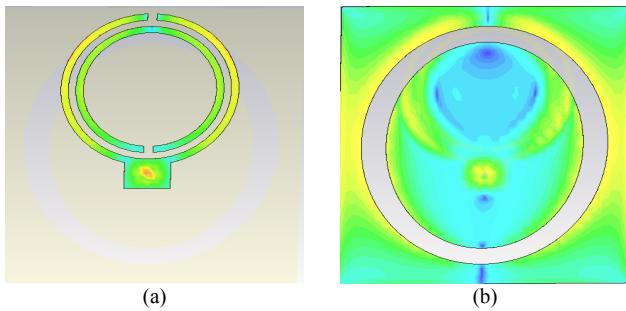


Fig. 6. The surface current distribution of the proposed energy harvesting antenna; (a) top and (b) bottom views.

The surface current distribution at the resonance frequency of 900 MHz is shown in Fig. 6. The resonance current distribution indicates the operation principle of the antenna, which is in the form of  $\lambda$  resonance characteristic feature of capacitively coupled split-ring resonators on the upper surface of the antenna and slotted ground plane on the lower antenna surface in the form of electrical coupling in between.

The 3D radiation pattern of the proposed antenna is shown in Fig. 7. The halfpower beamwidth (HPBW) of the radiated field is more than 90 degrees (94.8 degrees) in azimuth plane with the peak gain of 3.42 dBi at 900 MHz.

The antenna radiation efficiency is 96.3% with the directivity of 3.61 dBi. The alternative energy harvesting antenna designs in the literature are listed in Tab. 3 to point out the comparative better radiation performance of the proposed antenna design.

The RF terminal performance of the proposed antenna is numerically studied to determine how much input power can be gathered in the receiving mode as shown in the experimental setup model in Fig. 8.

In order to model the experimental setup, antenna feeding port is replaced by the lumped element as the port termination. The ambient radiating field is modeled as the plane wave excitation in a far field region with the separation distance of 500 mm from the antenna. In Fig. 9, the terminal voltage and current values on the antenna lumped port are shown for the input power level of -11 dBm.

At the resonance frequency of 900 MHz, the terminal voltage of 88.4 mV and current of 1.77 mA are obtained which indicates the approximately -11 dBm power to be

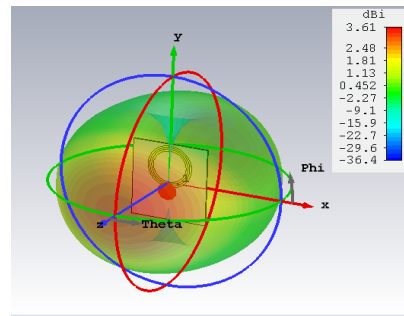


Fig. 7. The 3D radiation pattern of the proposed energy harvesting antenna at the resonance frequency of 900 MHz.

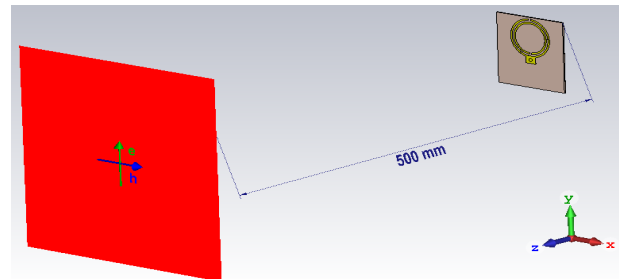


Fig. 8. Antenna measurement setup.

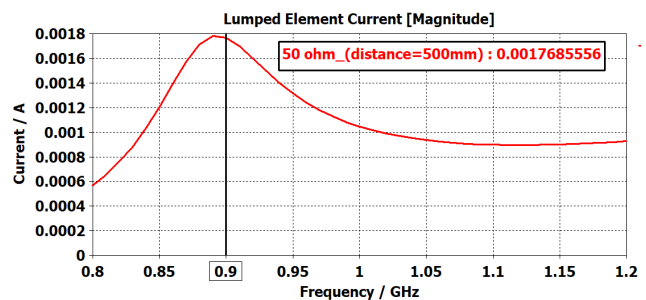
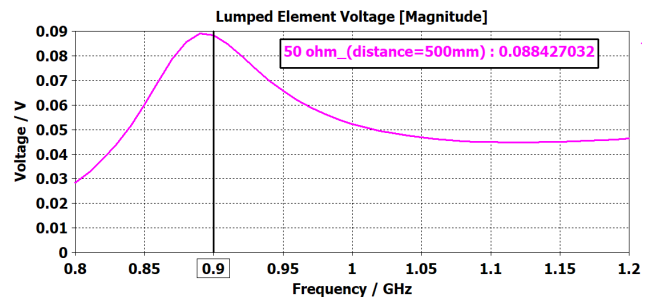


Fig. 9. Terminal voltage and current values on the antenna input port.



	Physical Dimensions [mm]	Directivity	Radiation Efficiency (Total Efficiency)	Center Frequency (Bandwidth)	Gain	Operating Frequency Band
Ref [26]	120 × 55 0.5 (thickness)	1.8 dBi	84%	915 MHz (300 MHz) (30.3%)	2.05 dBi	850–1150 MHz
Ref [27]	128 × 109.6 0.8 (thickness)	2.5 dBi	60.75%	848 MHz (21 MHz) (1.9%)	2.29 dBi	839–860 MHz
Ref [12]	3 dBi Commercial Antenna	Unspecified	Unspecified	878 MHz (47 MHz) (4%)	3 dBi	856–903 MHz
Ref [28]	120 × 50 1.6 (thickness)	Unspecified	Unspecified	915 MHz (124 MHz) (13.6%)	1.97 dBi	853–977 MHz
This work	81.25 × 87.5 1.524 (thickness)	3.60 dBi	96.3% (94.5%)	900 MHz (34.6 MHz) (3.4%)	3.35 dBi	886.3–920.9 MHz

Tab. 3. Proposed energy harvesting antenna performance with the alternative antenna designs in literature.

obtained by the energy harvesting antenna in the receiving mode. It is also important to figure out how much the incident RF power is being transferred into the RF load termination of the proposed antenna for the determination of the amount of RF power to be converted into DC power at DC load in the energy harvesting system. This figure of merit, RF power capturing efficiency ( $\eta_{cap}$ ), can be calculated as the ratio of RF power at the output load termination to the incident power received by the antenna [29].

$$\eta_{cap} = \frac{P_{out}}{P_{inc}} \tag{1}$$

$P_{out}$  is the total time-average power developed across the antenna termination load and calculated as

$$P_{load} = \frac{|V_{terminal}| \cdot |I_{terminal}|}{2} \tag{2}$$

$P_{inc}$  is the total time-average power incident on the antenna and calculated as

$$P_{inc} = \frac{|E_{inc}|^2 A_{eff}}{2Z_0} \tag{3}$$

where  $E_{inc}$  is the electric field amplitude of incident plane wave,  $A_{eff}$  is the effective area of the receiving antenna,  $Z_0$  is the free space wave impedance.

The RF power capturing efficiency of the proposed antenna is computed as 35.86%.  $\eta_{cap}$  can be improved by the use of periodic arrangement of unit cells in the form of metamaterial RF absorbers with the metal backing at the lower substrate side instead of slotted elliptical ring.

The RF-DC rectification performance of the RF energy harvesting module has been pointed out with the numerical computations in the commercial RF electronic circuit design software, Ansoft Designer. The RF-DC conversion efficiency and input impedance matching of the RF-DC rectifier circuit in Fig. 3 are shown in Fig. 10. As shown in Fig. 9(b), even though the input impedance of the RF-DC rectifier circuit is matched to the antenna input impedance of 50  $\Omega$  in 900 MHz band for –30 dBm input power level, the best RF-DC conversion efficiency is observed with the maximum value of 75% for the input

power level of –11 dBm as shown in Fig. 10(a). Therefore, the output DC voltage level depending on the DC load resistance is determined at the optimum input power level of –11 dBm where the maximum RF-DC conversion efficiency has been obtained. As shown in Fig. 11, the output DC voltage is increased to higher value with the larger load resistance for the same input power level. However, as a result of input impedance mismatch of the RF-DC rectifier circuit and power distribution in the generated higher order harmonics in the Schottky barrier diodes for different load resistances, the output voltage is not increased proportionally to the square root of load resistance for the same input power. As shown in Fig. 11, the output voltage level is higher than 1 V for the input power level more than –15 dBm (30  $\mu$ W).

DC voltage level can be increased sufficiently to operate any low power and low voltage electronic devices with the use of antenna arrays. To figure out the time domain

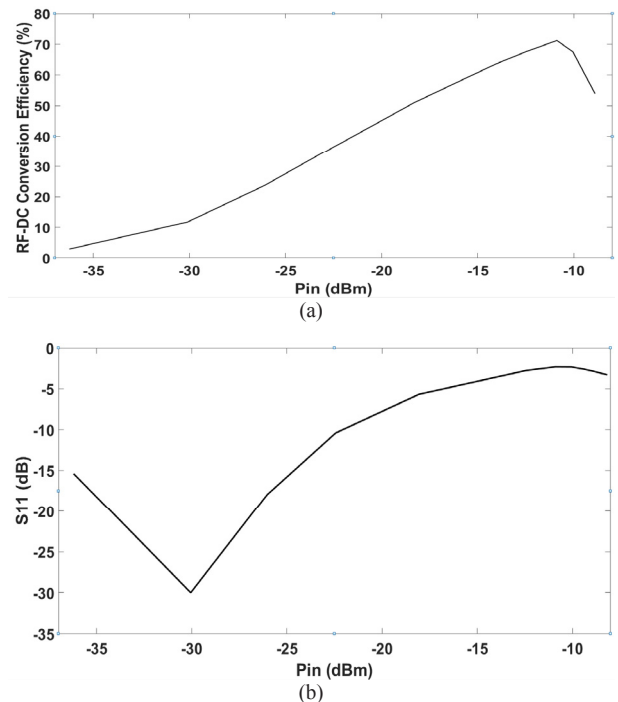
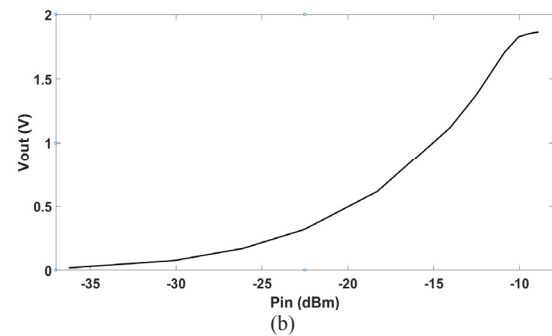
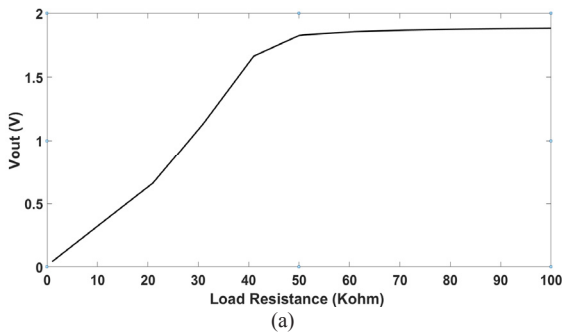
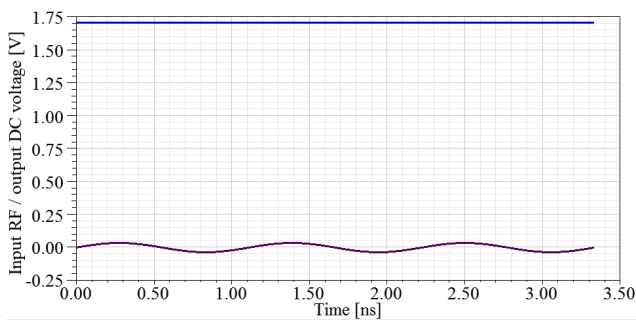


Fig. 10. RF-DC conversion efficiency and reflection coefficient (S11) of RF-DC rectifier at the resonance frequency.



**Fig. 11.** DC output voltage level depending on different DC load resistance and RF input power level at the resonance frequency.



**Fig. 12.** RF input and DC output voltage values of the proposed rectifying circuit for  $-11$  dBm input power level.

rectification feature of RF-DC rectifier circuit, the input RF signal and output DC voltage for  $-11$  dBm input power are shown in Fig. 12. The RF signal amplitude and DC output voltage value are 28 mV and 1.7 V, respectively.

## 4. Conclusion

In this paper, a rectenna design consisting of a probe fed SRR on the elliptical slotted ground plane in conjunction with RF-DC rectifying unit is proposed and numerically investigated for the energy harvesting applications at 900 MHz. The nonlinear modeling and systematic optimization of the proposed rectenna have been performed as a whole complete system. The numerical and experimental results indicate the proposed rectenna to generate 1.7 V DC output voltage at the center frequency of 900 MHz for  $-11$  dBm input power. Therefore, the technical potential of the proposed rectenna system has been numerically and experimentally confirmed for the operation of any low

power electronic devices with the improved capture efficiency in antenna arrays.

## Acknowledgement

This work was supported by Izmir Katip Celebi University BAP Office (Scientific Research coordinatorship of IKCU) under the Grant Number 2016-ÖNP-MÜMF-0029.

## References

- [1] PAVONE, D., BUONANNO, A., D'URSO, M., et al. Design considerations for radio frequency energy harvesting devices. *Progress In Electromagnetics Research Journal*, 2012, vol. 45, p. 19–35. DOI: 10.2528/PIERB12062901
- [2] LU, X., WANG, P., NIYATO, D., et al. Wireless networks with RF energy harvesting: A contemporary survey. *IEEE Communications Surveys and Tutorials*, 2014, vol. 17, no. 2, p. 757–789. DOI: 10.1109/COMST.2014.2368999
- [3] KIM, J. H., BITO, J., TENTZERIS, M. M. Design optimization of an energy harvesting rf-dc conversion circuit operating at 2.45 GHz. In *IEEE International Symposium on Antennas and Propagation and USNC/URSI National Radio Science Meeting*. Vancouver (BC, Canada), 2015. DOI: 10.1109/APS.2015.7305029
- [4] ZAKARIA, Z., ZAINUDDIN, N. A., HUSAIN, M. N., et al. Current developments of RF energy harvesting system for wireless sensor networks. *International Journal on Advances in Information Sciences and Service Sciences (AISS)*, 2013, vol. 5, no. 11, p. 328–338. DOI: 10.4156/AISS.vol5.issue11.39
- [5] PENELLA-LOPEZ, M. T., GASULLA-FORNER, M. *Powering Autonomous Sensors: An Integral Approach with Focus on Solar and RF Energy Harvesting*. 1st ed. Barcelona: Springer Science + Business Media, 2011. Chapter 6. ISBN 978-94-007-1573-8
- [6] AGRAWAL, S., PANDEY, S., SINGH, J., et al. An efficient RF energy harvester with tuned matching circuit. In *VLSI Design and Test, 17th International Symposium, VDAT*. Jaipur (India), 2013, vol. 382, p. 138–145. DOI: 10.1007/978-3-642-42024-5\_17
- [7] MUNIR, S. W., AMJAD, O., ZEYDAN, E., et al. Optimization and analysis of WLAN RF energy harvesting system architecture. In *2016 International Symposium on Wireless Communication Systems (ISWCS)*. Poznan (Poland), 2016, p. 429–433. DOI: 10.1109/ISWCS.2016.7600942
- [8] RAZAVI HAERI, A. A., GHADERI KARKANI, M., SHARIFKHANI, M., et al. Analysis and design of power harvesting circuits for ultra-low power applications. *IEEE Transactions on Circuits and Systems I: Regular Papers*, 2017, vol. 64, no. 2, p. 471–479. DOI: 10.1109/TCSL.2016.2609144
- [9] MATTSSON, M., KOLITSIDAS, C. I., SILVER, O. B. G., et al. A high gain dual-polarised differential rectenna for RF energy harvesting. In *2017 IEEE International Symposium on Antennas and Propagation & USNC/URSI National Radio Science Meeting*. San Diego (CA, USA), 2017, p. 1609–1610. DOI: 10.1109/APUSNCURSINRSM.2017.8072847
- [10] SARMA, S. S., AKHTAR, M. J. A dual band meandered printed dipole antenna for RF energy harvesting applications. In *2016 IEEE 5th Asia-Pacific Conference on Antennas and Propagation (APCAP)*. Kaohsiung (Taiwan), 2016, p. 93–94. DOI: 10.1109/APCAP.2016.7843115

- [11] CHANG, M. C., WENG, W. C., CHEN, W. H., et al. A wideband planar rectenna for WLAN wireless power transmission. In *2017 IEEE Wireless Power Transfer Conference (WPTC)*. Taipei (Taiwan), 2017, p. 1–3. DOI: 10.1109/WPT.2017.7953823
- [12] ZAKARIA, Z., ZAINUDDIN, N. A., ABD AZIZ, M. Z. A., et al. Dual-band monopole antenna for energy harvesting system. In *2013 IEEE Symposium on Wireless Technology & Applications (ISWTA)*. Kuching (Malaysia), 2013, p. 225–229. DOI: 10.1109/ISWTA.2013.6688775
- [13] MAVADDAT, A., ARMAKI, S. H. M., ERFANIAN, A. R. Millimeter-wave energy harvesting using 4times4 microstrip patch antenna array. *IEEE Antenna Wireless Propagation Letters*, 2014, vol. 14, p. 515–518. DOI: 10.1109/LAWP.2014.2370103
- [14] YO, T.-C., LEE, C.-M., HSU, C.-M., et al. Compact circularly polarized rectenna with unbalanced circular slots. *IEEE Transactions on Antennas and Propagation*, 2008, vol. 56, no. 3, p. 882–886. DOI: 10.1109/TAP.2008.916956
- [15] HEIKKINEN, J., KIVIKOSKI, M. A novel dual-frequency circularly polarized rectenna. *IEEE Antenna Wireless Propagation Letters*, 2003, vol. 2, p. 330–333. DOI: 10.1109/LAWP.2004.824166
- [16] PALANDOKEN, M. Microstrip antenna with compact anti-spiral slot resonator for 2.4 GHz energy harvesting applications. *Microwave and Optical Technology Letters*, 2016, vol. 58, no. 6, p. 1404–1408. DOI: 10.1002/mop.29824
- [17] TU, W.-H., HSU, S.-H., CHANG, K. Compact 5.8-GHz rectenna using stepped-impedance dipole antenna. *IEEE Antennas and Wireless Propagation Letters*, 2007, vol. 6, p. 282–284. DOI: 10.1109/LAWP.2007.898555
- [18] PALANDOKEN, M. Artificial materials based microstrip antenna design. Chapter in Nasimuddin, N. (ed.) *Microstrip Antennas*. InTechOpen, 2011. DOI: 10.5772/14908
- [19] BORATAY ALICI, K. B., OZBAY, E. Electrically small split ring resonator antennas. *Journal of Applied Physics*, 2007, vol. 101, no. 8, p. 1–4, ID 083104. DOI: 10.1063/1.2722232
- [20] BARBUTO, M., BILOTTI, F., TOSCANO, A. Design of a multifunctional SRR-loaded printed monopole antenna. *International Journal of RF and Microwave Computer Aided Engineering*, 2012, vol. 22, no. 4, p. 552–557. DOI: 10.1002/mmce.20645
- [21] BARBUTO, M., MONTI, A., BILOTTI, F., et al. Design of a non-foster actively loaded SRR and application in metamaterial-inspired components. *IEEE Transactions on Antennas and Propagation*, 2013, vol. 61, no. 3, p. 1219–1227. DOI: 10.1109/TAP.2012.2228621
- [22] CST MICROWAVE STUDIO CST, ver. 2017.00 [Online] Cited 2018-03-19 Available at <http://www.cst.com/products/cstmw/>.
- [23] ANSOFT CORPORATION, *Ansoft Designer*. [Online] Cited 2018-03-19. Available at [http://www.ansoft.com/products/hf/ansoft\\_designer/](http://www.ansoft.com/products/hf/ansoft_designer/).
- [24] SKYWORKS *SMS7630 Series' Technical Documentation*. [Online] Cited 2018-03-19 Available at [http://www.skyworksinc.com/Product/511/SMS7630\\_Series#three](http://www.skyworksinc.com/Product/511/SMS7630_Series#three)
- [25] *KY-028 Digital Temperature Sensor* [Online] Cited 2018-03-19 Available at [http://sensorkit.en.joy-it.net/index.php?title=KY028\\_Temperature\\_Sensor\\_module\\_\(Thermistor\)#Technical\\_data\\_2F\\_Short\\_description](http://sensorkit.en.joy-it.net/index.php?title=KY028_Temperature_Sensor_module_(Thermistor)#Technical_data_2F_Short_description).
- [26] TAVARES, J., BARROCA, N., SARAIVA, H. M., et al. Spectrum opportunities for electromagnetic energy harvesting from 350 MHz to 3 GHz. In *2013 7th International Symposium on Medical Information and Communication Technology (ISMICT)*. Tokyo (Japan), 2013, p. 126–130. DOI: 10.1109/ISMICT.2013.6521714
- [27] OSMAN, Z., AZEMI, S. N., EZANUDDIN, A. A. M., et al. Compact antenna design for outdoor RF energy harvesting in wireless sensor networks. In *2016 3rd International Conference on Electronic Design (ICED)*. Phuket (Thailand), 2016, p. 199–202. DOI: 10.1109/ICED.2016.7804636
- [28] TARIS, T., VIGNERAS, V., FADEL, L. A 900MHz RF energy harvesting module. In *10th IEEE International NEWCAS Conference*. Montreal (QC, Canada), 2012, p. 445–448. DOI: 10.1109/NEWCAS.2012.6329052
- [29] ALMONEEF, T. S., RAMAHI, O. M. Metamaterial electromagnetic energy harvester with near unity efficiency. *Applied Physics Letters*, 2015, vol. 106, no. 15, p. 1–4, ID 153902. DOI: 10.1063/1.4916232

## About the Authors ...

**Merih PALANDOKEN** (corresponding author) received M.Sc. degree in Microelectronics and Microsystems Engineering from the Technical University of Hamburg, Germany, in 2005; and Ph.D. degree in Theoretical Electrical Engineering from the Technical University of Berlin, Germany in 2012. He has been working in the analytical and numerical design and modeling of active/passive wireless components in the micro/millimeter wave frequencies, especially in the field of metamaterial-based antennas and microwave filters.

**Cem GOCEN** was born in Izmir in 1992. He received B.E. degree in Electrical and Electronics Engineering from Ankara University, Turkey, in 2016. He has been working on electromagnetic fields and microwave technique.

**Adnan KAYA** received M.Sc. degree in Electronic Communications Engineering from Süleyman Demirel University, in 1999; Ph.D. degree in Electrical Electronic Engineering from Dokuz Eylül University, in 2006. He has been working as a professor in the field of PEMF/PRF system design based on alternative RF signal generation techniques, emerging new generation wireless communication system technologies and dedicated wireless component and system design.

**Fethullah GUNES** received his combined M.Sc. and Ph.D. degree in the field of Nanoscience and Nanotechnology from Sung Kyun Kwan University, Republic of Korea (South) in 2011. His research interests include nanomaterials, graphene and 2D materials along with their electronic and biological applications.

**Cem BAYTORE** received his M.Sc. degree from Ege University in 2013. He has been studying for the doctorate at Dokuz Eylül University. His research interests include electromagnetic waves and microwave engineering.

**Fatih Cemal CAN** received his M.Sc. degree from the Middle East Technical University in 2003 and Ph.D. from İzmir Institute of Technology in 2009. His research interests include robotics, analysis and synthesis manipulators and mechatronic systems.